Self-Splicing of the Group I Intron from *Anabaena* Pre-tRNA: Requirement for Base-Pairing of the Exons in the Anticodon Stem†

Arthur J. Zaug, Megan M. McEvoy, and Thomas R. Cech*

Howard Hughes Medical Institute, Department of Chemistry and Biochemistry, University of Colorado, Boulder, Colorado 80309-0215

Received March 17, 1993; Revised Manuscript Received May 13, 1993

ABSTRACT: In the cyanobacterium *Anabaena*, the precursor to $tRNA^{Leu}$ has a 249-nucleotide group I intron inserted between the wobble and second bases of the anticodon; the intron self-splices during transcription in vitro [Xu, M. Q., Kathe, S. D., Goodrich-Blair, H., Nierzwicki-Bauer, S. A., & Shub, D. A. (1990) *Science 250*, 1566–1570]. By studying splicing of isolated pre-tRNA, we confirm that splicing occurs by the two-step transesterification mechanism characteristic of group I introns, resulting in excision of the intron and accurate ligation of the 5′ and 3′ exons. The first step, guanosine-dependent cleavage of the phosphodiester bond at the 5′ splice site, occurs with $k_{cat} \simeq 14$ min^{-1} and $k_{cat}/K_m = 5 \times 10^4$ M^{-1} min^{-1} (32 °C, 15 mM $MgCl_2$), unexpectedly efficient for a small group I intron. (k_{cat}/K_m is comparable to that of the *Tetrahymena* pre-rRNA intron, and k_{cat} is an order of magnitude higher than any previously reported for a group I intron.) The second step, ligation of the exons, is so slow ($k = 0.3$ min^{-1}) that it is rate-limiting for splicing in vitro except at very low guanosine concentrations. Disruption of the base pairs that make up the anticodon stem of the tRNA dramatically reduces the rate of the first step of splicing, while compensatory mutations that restore base pairing generally restore activity. We suggest that the very short P1 helix of this pre-tRNA, with only three base pairs preceding the 5′ splice site, is unstable without the additional base pairs in the anticodon stem. Thus, splicing of the *Anabaena* pre-tRNA involves collaboration of the intron and tRNA structures.

Group I introns are distributed widely across phylogenetic boundaries (Michel & Dujon, 1983; Waring et al., 1983). In eukaryotes, they have been found in the nuclei of the ciliate *Tetrahymena* (Wild & Gall, 1979), the fungi *Physarum* (Nomiyama et al., 1981) and *Pneumocystis* (Sogin & Edman, 1989), and the green alga *Ankistrodesmus stipitatus* (Davila-Aponte et al., 1991). They exist in the mitochondria of yeast and other fungi [e.g., Garriga and Lambowitz (1984) and van der Horst and Tabak (1985)] and in the chloroplasts of *Chlamydomonas* and higher plants. Group I introns have also been found in bacteriophage T4 (Chu et al., 1986; Gott et al., 1986). Recently they were found in *Anabaena* and other cyanobacteria, which are the proposed progenitors of chloroplasts (Kuhsel et al., 1990; Xu et al., 1990).

All group I introns share a common secondary structure. Their 5′ splice site is in a paired (helical) region designated P1, and their catalytic core includes a series of helical regions numbered P3 through P9 (Burke et al., 1987; Davies et al., 1982; Michel et al., 1982). The catalytic core contains nucleotides that are directly involved in binding the guanosine (G)[1] substrate, which acts as a nucleophile in the first step of splicing (Michel et al., 1989). It also contains nucleotides that position the P1 helix for attack by guanosine and contribute in other ways to active site chemistry (Pyle et al., 1992; Cech et al., 1992). Outside the core region, sequence and structural elements can vary greatly among group I introns and still be compatible with self-splicing activity.

The group I intron from *Anabaena* (Figure 1A) differs structurally from group I introns that are known to self-splice efficiently in vitro under physiological Mg^{2+} concentrations. In contrast to the *Tetrahymena* intron, the *Anabaena* intron has no P2.1 or P5abc, and its P9 region is quite different. Deletion of any of these structural elements from the *Tetrahymena* group I intron abolishes or greatly reduces splicing activity (Price et al., 1985; Barfod & Cech, 1988; Beaudry & Joyce, 1990; van der Horst et al., 1991). Furthermore, although the efficiently spliced phage T4 introns do not have P2.1 or the P5abc extension, they have additional elements, P7.1 and 7.2, which aid in splicing (Doudna & Szostak, 1989). None of these elements is present in the *Anabaena* intron. The P10 pairing is one of several interactions that align the 3′ splice site for the second step of splicing (Davies et al., 1982; Michel et al., 1989; Suh & Waring, 1990). It consists of seven base pairs in the *Tetrahymena* intron and two or three base pairs in the phage T4 introns. In contrast, the P10 pairing, if it exists at all in the group I intron from *Anabaena* PCC7120, would consist of two AU base pairs, or one base pair in another species, *Anabaena azollae* (Xu et al., 1990). In group I introns, the 5′ exon is positioned for splicing in part by its base-pairing to the internal guide sequence (IGS), forming the P1 duplex (Davies et al., 1982; Michel et al., 1982). The median number of base pairs preceding the 5′ splice site in P1 is five, with a range of three to eight base pairs in a compilation of 87 group I introns (Michel & Westhof, 1990). In the *Tetrahymena* group I intron, where there are normally six base pairs, shortening P1 decreases guanosine addition at the 5′ splice site (Doudna et al., 1989). The group I intron from *Anabaena* has a short P1 helix, with only three base pairs preceding the 5′ splice site.

Considering that the group I intron from the *Anabaena* intron is missing internal structural elements and has abnormally short P1 and P10 helices, it seemed likely to us that it would splice inefficiently in the absence of protein in vitro. Consistent with such an expectation, the pre-$tRNA^{Leu}$ group

†A.J.Z. is a Senior Associate and T.R.C. is an Investigator of the Howard Hughes Medical Institute. T.R.C. is also an American Cancer Society Professor.

*Author to whom correspondence should be addressed.

[1] Abbreviations: G, guanosine; k_{cat}, maximum rate of the first step of splicing (G-addition) at saturating concentrations of G.

0006-2960/93/0432-7946$04.00/0

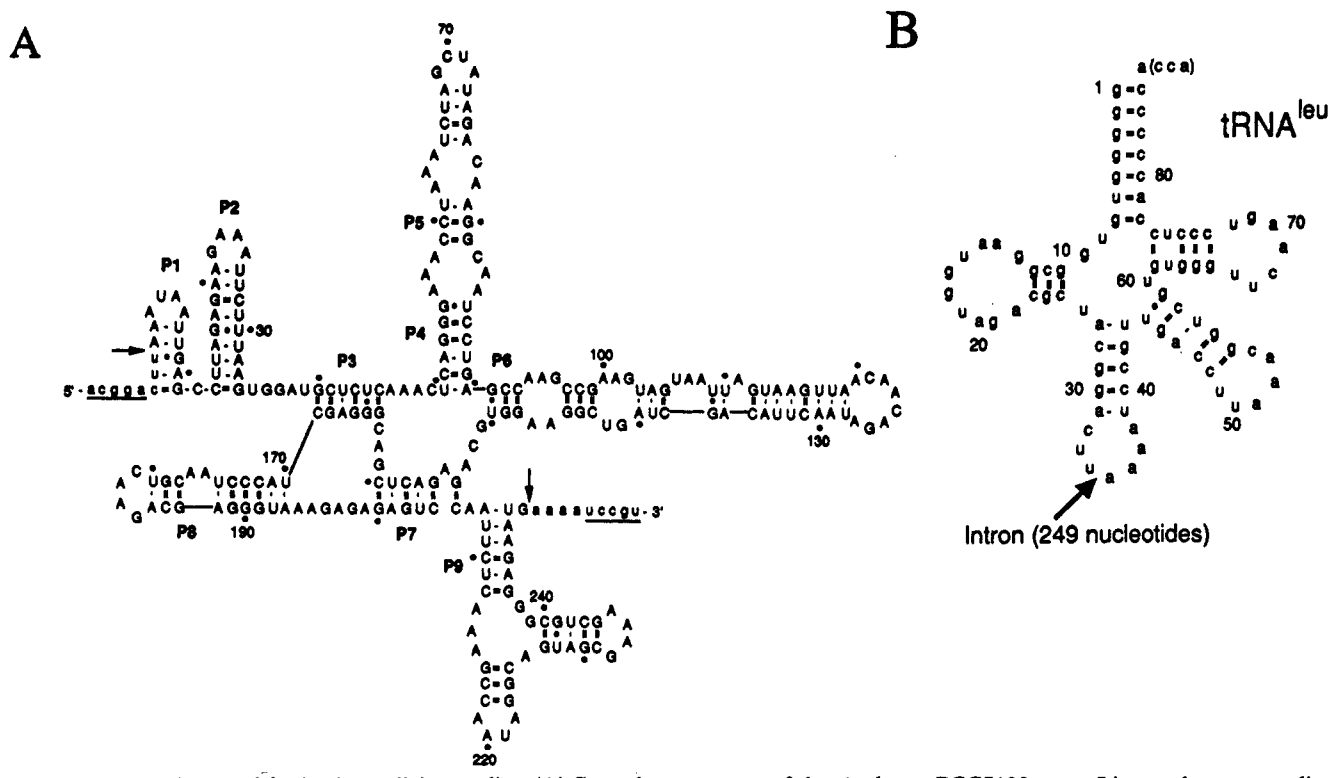

FIGURE 1: Pre-tRNA used for in vitro splicing studies. (A) Secondary structure of the *Anabaena* PCC7120 group I intron drawn according to convention (Burke et al., 1987). Paired regions P1–P9 are indicated. Exon sequences are in lowercase, and intron sequences are in uppercase. The 5′ and 3′ splice sites are indicated by arrows. Underlined exon sequences indicate the regions of base-pairing in the $tRNA^{Leu}$ anticodon stem. (B) Secondary structure of leucine tRNA. The intron is inserted between bases 34 and 35 of the tRNA as indicated by the arrow. The parentheses around cca indicate that these 3′-terminal nucleotides were not present in the precursor studied here.

I introns of plant chloroplasts, which have nucleotide sequences highly similar to that of the *Anabaena* intron, do not self-splice (Xu et al., 1990). We have now measured the catalytic activity of the *Anabaena* intron. Surprisingly it has a k_{cat}/K_m similar to that of the *Tetrahymena* group I intron and a k_{cat} more than 10-fold higher. Furthermore, studies of mutants in the 5′ and 3′ exons of this precursor indicate that the anticodon stem of the tRNA precursor contributes significantly to splicing activity. We propose that the tRNA anticodon stem helps compensate for the short P1 and lack of a significant P10 interaction in this precursor.

MATERIALS AND METHODS

Plasmid Construction. Genomic clone pXAb-107 was a gift from David Shub and was constructed by inserting a 1.2-kb *Hin*dIII genomic fragment which contained the leucine tRNA gene from *Anabaena* PCC7120 into the *Hin*dIII site of pBS(−) (Stratagene) in the T7 promoter orientation. Exon sequence and length can affect the rate of splicing of the *Tetrahymena* pre-rRNA in vitro (Bass & Cech, 1986; Woodson & Cech, 1991). To eliminate extra sequences that might affect splicing of the pre-tRNA in vitro, 870 base pairs of DNA between the T7 promoter and the coding region of the $tRNA^{Leu}$ gene were deleted. In addition, an *Ear*I restriction endonuclease site was inserted just beyond the 3′ end of the tRNA gene to allow linearization of the plasmid to provide a termination site for T7 RNA polymerase. The resulting plasmid, pAtRNA-1, when transcribed with T7 RNA polymerase, produces a primary transcript of 334 nucleotides, consisting of a 40-base 5′ exon, which begins at base 1 of the mature tRNA; a 249-base intron; and a 45-base 3′ exon, which ends immediately prior to the CCA sequence (Figure 1).

Mutagenesis. All mutants described were constructed using oligonucleotide-directed mutagenesis (Kunkel et al., 1987). DNA oligonucleotides were synthesized on an Applied Biosystems 380B DNA synthesizer, phosphorylated using ATP and T4 polynucleotide kinase (New England Biolabs), and subsequently annealed to deoxyuridine-containing single-stranded circular DNA. Second-strand synthesis was initiated by the addition of dNTPs, T4 DNA polymerase (U.S. Biochemical Corp.), and T4 DNA ligase (U.S. Biochemical Corp.). Resultant double-stranded DNA was used to transform competent *Escherichia coli* JM109 using a Bio-Rad gene pulser set at 1.8 kV and 400 Ω. Mutants were screened using restriction endonuclease digestion and sequencing (USB Sequenase kits). Mutants G29C, C41G, A31U, and U39A all have single point mutations in the anticodon stem of the tRNA (see Figure 1B). 5′-Anti and 3′-anti mutants disrupt all base-pairing in the anticodon stem. Compensatory double mutants G29C:C41G, A31U:U39A, and 5′-anti:3′-anti restore base-pairing in the anticodon stem of the pre-tRNA.

Transcription of Precursor RNA. Due to the high splicing activity of the intron under standard transcription conditions, the $MgCl_2$ concentration was lowered and the ribonucleoside triphosphate (NTP) concentrations were raised to a level where the NTPs chelate most of the $MgCl_2$. This completely inhibited splicing during transcription (Michel et al., 1992). Transcription reaction mixtures (20 μL) for preparing uniformly labeled RNA contained 40 mM Tris-HCl (pH 7.5), 5 mM $MgCl_2$, 10 mM DTT, 2 mM spermidine, 4 mM each NTP, 1 μg of DNA template cleaved with *Ear*I, 50 μCi of [α-^{32}P]ATP (New England Nuclear), and 2000 units of T7 RNA polymerase (activity determined relative to polymerase from U.S. Biochemical Corp.). After addition of polymerase, the mixture was incubated at 37 °C for 1 h. RNA was purified by electrophoresis on 6% polyacrylamide [29:1 acrylamide:bis(acrylamide)]/8 M urea gels. The gel slice was crushed and then soaked in 10 mM Tris-HCl (pH 7.5), 1 mM EDTA, and 250 mM NaCl, which was followed by removal of the polyacrylamide by filtration and subsequent ethanol precip-

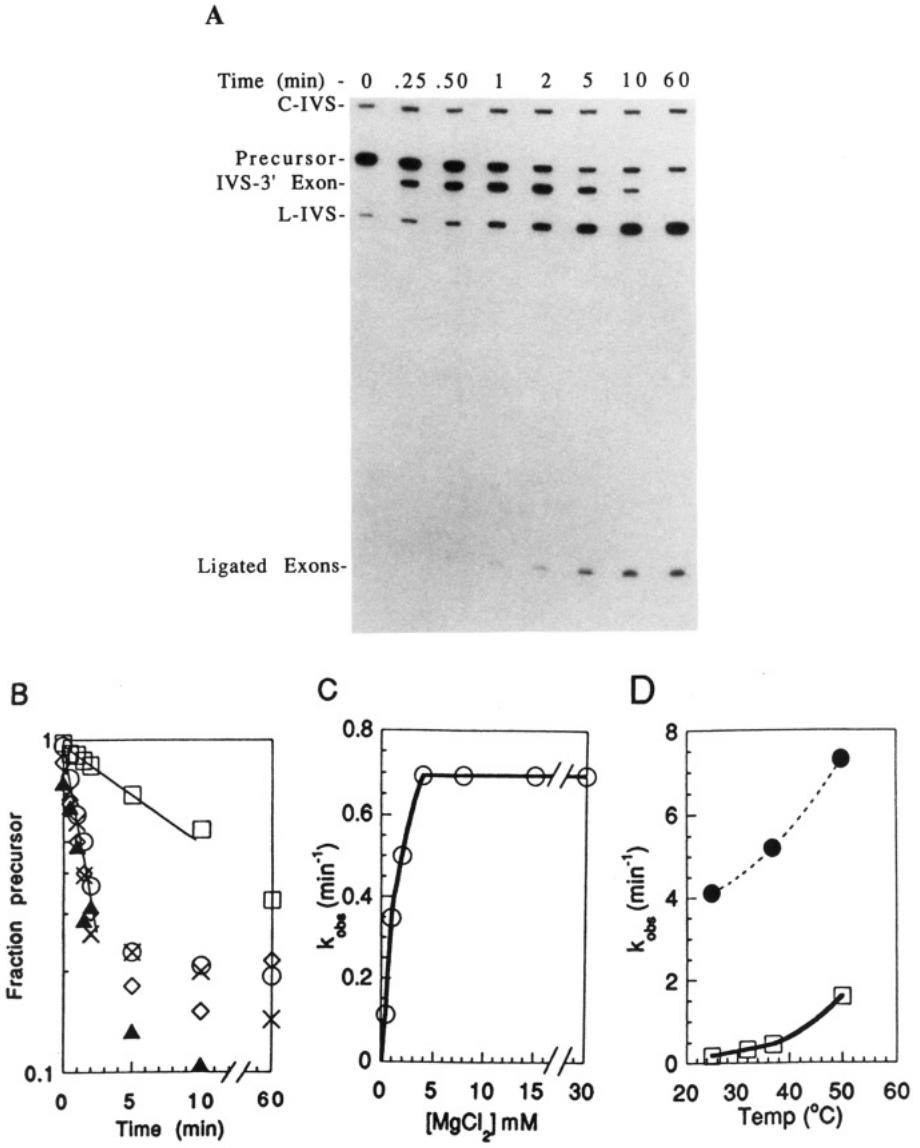

FIGURE 2: Characterization of self-splicing of *Anabaena* pre-tRNA^{Leu}. (A) Splicing of uniformly ^{32}P-labeled pre-tRNA. At time point 0, the precursor has gone through preincubation for 15 min at 50 °C and 2 min at 32 °C in 25 mM Hepes (pH 7.5) and 15 mM $MgCl_2$. During this preincubation, a portion of the precursor undergoes G-independent reactions, forming a circular intron (C-IVS) and a linear intron (L-IVS; see text). Splicing was initiated by the addition of guanosine (final concentration of 25 μM) at 32 °C. Portions of the reaction mixture were removed at the indicated times, stopped, and analyzed by polyacrylamide gel electrophoresis. (B) Renaturation of pre-tRNA by preincubation at 50 °C: semi-log plot of the fraction of precursor (pre-tRNA) remaining vs time (min), varying the time of preincubation at 50 °C. Pre-tRNA was incubated at 50 °C in the presence of 15 mM $MgCl_2$ and 25 mM Hepes (pH 7.5) for 0 (□), 2 (○), 10 (×), 20 (◇), or 60 min (▲). After the preincubation, the temperature was reduced to 37 °C for 2 min, and splicing was initiated by the addition of guanosine (10 μM final concentration). Time points were taken at 0, 0.25, 0.5, 1, 2, 5, 10, and 60 min. Unlike the subsequent analyses, no normalization for the fraction of precursor unreacted was performed in this initial experiment. (C) $MgCl_2$ dependence: pseudo-first-order rate constant for the first step of splicing (k_{obs}) vs $MgCl_2$ concentration. Pre-tRNA was preincubated at 50 °C for 20 min and then at 37 °C for 2 min in 25 mM Hepes (pH 7.5) and 15 mM $MgCl_2$. Before the addition of guanosine to initiate splicing, the $MgCl_2$ concentration was adjusted by dilution or addition. k_{obs} was calculated for each $MgCl_2$ concentration from first-order plots similar to that shown in B. (D) Temperature dependence. Precursor was preincubated as usual for 15 min at 50 °C and then at the reaction temperature of 25, 32, 37, or 50 °C for an additional 2 min. Splicing was initiated by the addition of guanosine (250 μM final concentration). •, k_{obs} for the first step of splicing calculated as in C. □, k_{obs} for the second step of splicing determined by monitoring the conversion of IVS-3′ exon into L-IVS and ligated exons.

itation. Purified RNA was dissolved in a small amount of H_2O (50–100 μL), and a 1-μL portion was counted in a scintillation counter. T7 RNA polymerase was isolated from *E. coli* strain BL21 containing the plasmid pAR1219 (Davanloo et al., 1984).

Splicing Reactions. Uniformly ^{32}P-labeled precursor was preincubated in 25 mM Hepes (pH 7.5) and 15 mM $MgCl_2$ at 50 °C for 15 min and then at 32 °C for 2 min. Splicing was initiated by the addition of guanosine (0–2000 μM) in the same buffer at 32 °C, unless otherwise indicated. Portions were removed at indicated times, and the splicing reaction was stopped by the addition of an equal volume of a stop mix consisting of 30 mM EDTA, 10 M urea, 0.01% bromophenol blue, 0.025% xylene cyanol, and 0.1× Tris–borate–EDTA electrophoresis buffer (1× TBE is 0.1 M Tris base, 0.083 M boric acid, and 1 mM EDTA). Samples were run on 6% polyacrylamide/8 M urea gels, subjected to autoradiography, and quantitated by direct scanning of radioactivity (Ambis system). The data were first plotted as log F vs t, where F = fraction of precursor remaining = $p/(p + 3' + i + le)$; p = counts in pre-tRNA, 3′ = counts in IVS-3′ exon, i = counts in L-IVS, and le = counts in ligated exons. The kinetics were biphasic, with the majority of the RNA reacting at the faster rate. The fraction reacting in the slow transition was determined (F_{slow}; typically 20% of the total precursor) and used to normalize the data to consider the more active

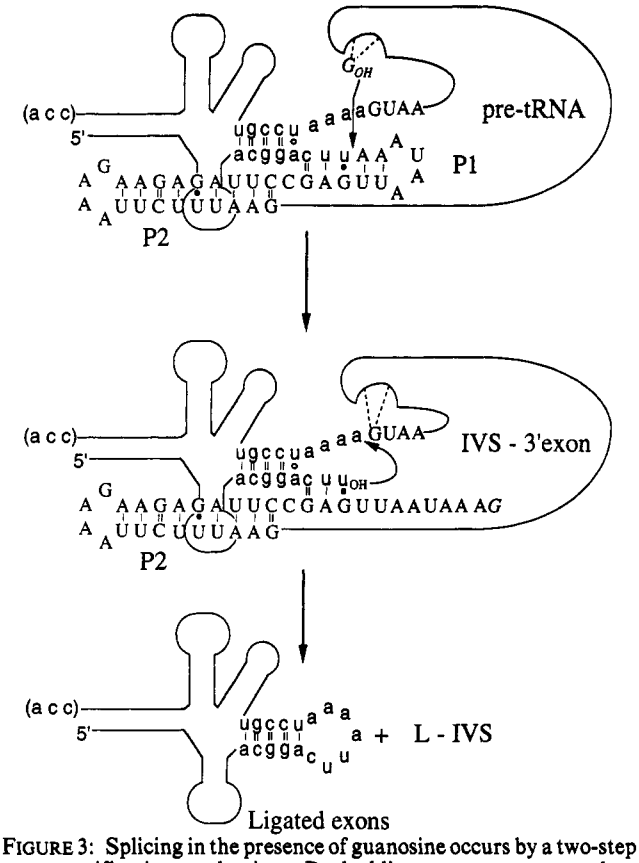

FIGURE 3: Splicing in the presence of guanosine occurs by a two-step transesterification mechanism. Dashed lines represent noncovalent interactions of exogenous guanosine (*G*) or the 3′-terminal guanosine of the intron with the guanosine-binding site in the intron. Arrows show positions of attack by hydroxyl groups. Capital letters, intron nucleotides; lowercase, exons. Neither the anticodon stem nor the P2 helix is shown as stacked on the P1 helix, because the structure was not directly investigated in the current study.

population only: Fraction of precursor (normalized) = $(F - F_{slow})/(1 - F_{slow})$. The slopes of the lines on the semi-log plots were taken as k_{obs}, or k_{obs} was calculated as $0.693/t_{1/2}$.

RESULTS

Characterization of Splicing. Unspliced pre-tRNA consisting of the $tRNA^{Leu}$ exons plus the intron was synthesized by transcription in vitro. An excess of nucleoside triphosphates over $MgCl_2$ was used to inhibit splicing during transcription [as described by Michel et al. (1992)]. Self-splicing was then monitored by gel electrophoresis as shown in Figure 2A. At time 0, the precursor has gone through a 15-min preincubation at 50 °C in splicing buffer without guanosine. A circular form of the intron (C-IVS) is produced during preincubation by hydrolysis at the 3′ splice site and subsequent circularization to the 5′ splice site of the precursor (data not shown). The C-IVS does not accumulate once the temperature is lowered to 32 °C and guanosine is added to initiate splicing, and thus it is not considered a product of splicing. Once guanosine is added, the precursor is converted into a series of faster migrating products typical of group I intron splicing (Cech & Bass, 1986; Figure 3). The formation of ligated exons (i.e., $tRNA^{Leu}$) was confirmed by dideoxy sequencing using reverse transcriptase, sequencing across the junction between the 5′ and 3′ exons (data not shown). The linear excised intron (L-IVS) and the splicing intermediate (IVS-3′ exon) were identified by their mobility relative to molecular weight markers. As expected for a reaction intermediate, the IVS-3′ exon accumulates early in the reaction and disappears as it is converted to the products of splicing, the L-IVS and ligated exons.

Catalytic RNAs are often in relatively inactive conformations after purification by denaturing gel electrophoresis and can be restored to active form by preincubation at elevated temperatures in the presence of $MgCl_2$ (Walstrum & Uhlenbeck, 1990; Herschlag & Cech, 1990). As shown in Figure 2B, preincubation of the *Anabaena* pre-tRNA at 50 °C in the presence of $MgCl_2$ for times ranging from 2 to 60 min increases the initial rate of splicing compared to precursor that was not preincubated at the elevated temperature (open squares in Figure 2B). Longer times of preincubation do not increase the initial rate of splicing; although the total fraction of precursor reacted in 10 min increases, this occurs at the expense of more precursor being lost by site-specific hydrolysis during the preincubation (note the decrease in the amount of precursor at time 0 in Figure 2B). The fraction of precursor which does not react at this faster initial rate (~20%) continues to react at a rate which is considerably slower and is similar to the initial rate seen when the precursor is not preincubated at 50 °C. A preincubation time of 15 min was chosen to ensure activation of the RNA.

Catalytic activity of the *Anabaena* intron increases with increasing $MgCl_2$ concentration between 0 and 4 mM (Figure 2C). Higher $MgCl_2$ concentrations up to 60 mM neither increase nor inhibit activity. Although the rate of splicing increases at higher temperatures (Figure 2D), the physiological temperature of 32 °C was chosen as the standard splicing condition to allow comparison of the in vitro results reported in this article with in vivo experiments.

Varying the concentration of NaCl in the splicing reaction mixture has only a modest effect on the rate of splicing of the pre-tRNA (data not shown). At 15 mM $MgCl_2$, addition of 250 mM NaCl increased the rate 1.5-fold compared to no added NaCl. Above 250 mM NaCl, the rate of splicing decreased. This is in contrast to the large increase in activity with high monovalent cation concentration observed with group I introns from bacteriophage T4 (*sun*Y and *nrd*B) and *A. stipitatus* (Hicke et al., 1989; Davila-Aponte et al., 1991).

Kinetic Parameters. The rate constant for the first step of splicing was measured at guanosine concentrations of 0–1000 μM by monitoring the disappearance of precursor with time (Figure 4A). At each guanosine concentration, the reaction followed pseudo-first-order kinetics as evidenced by the linear semi-log plot. The slopes of these lines were used to calculate k_{obs}, which increased linearly with guanosine concentration between 0 and 25 μM. At guanosine concentrations ≥100 μM, saturation behavior became apparent as a nonlinear increase in rate with an increase in guanosine concentration (Figure 4B). Although the rate of splicing became too fast to measure accurately at near-saturating concentrations of guanosine, the values of K_m = 240 μM and k_{cat} = 14 min^{-1} could be obtained by fitting the data of Figure 4B with the Michaelis–Menten equation. Because of the possibility of systematic error in taking short time points, it is possible that we are underestimating the rate of reaction at high [G], in which case $k_{cat} > 14$ min^{-1} and $K_m > 240$ μM. The second-order rate constant k_{cat}/K_m calculated from the slope of the line between 0 and 25 μM guanosine (inset in Figure 4B) is 4.6×10^4 M^{-1} min^{-1}. As listed in Table I, k_{cat}/K_m was moderately temperature-dependent, increasing by a factor of 2 from 25 to 37 °C.

In the absence of guanosine, the reaction was so slow that it was difficult to measure ($k \simeq 3 \times 10^{-4}$ min^{-1} at 32 °C). This minor reaction represented 3′ splice site hydrolysis, as first characterized for the *Tetrahymena* pre-rRNA by Inoue et al. (1986).

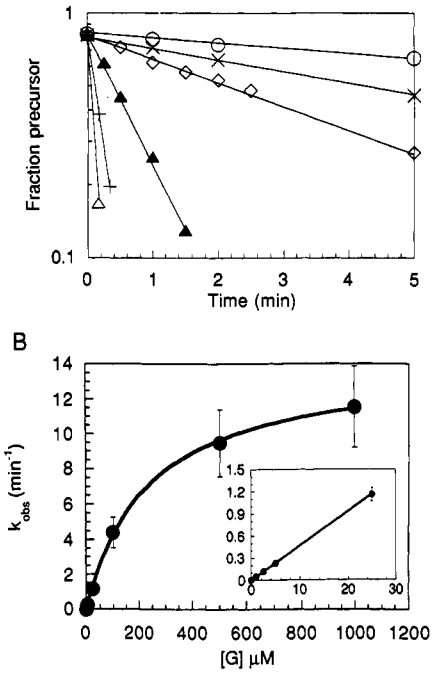

FIGURE 4: Kinetic analysis of the first step of splicing at 32 °C. (A) Semi-log plot showing the disappearance of precursor with time at guanosine concentrations of 1 (○), 2.5 (×), 5 (◇), 25 (▲), 100 (+), and 500 μM (△). (B) Plot of k_{obs} vs guanosine concentration. $k_{obs} = 0.693/t_{1/2}$ was calculated from the first-order plots in (A). Error bars represent the maximum and minimum slopes of the first-order plots, except for values of $k_{obs} > 8$ min^{-1} where they represent an estimated ±2-s uncertainty for a 10-s time point. The line is theoretical for the Michaelis–Menten equation ($k_{cat} = 14$ min^{-1}; $K_m = 240$ μM). (Inset) Determination of k_{cat}/K_m. Axes are the same as in (B). Slope of line = k_{cat}/K_m.

Table I: Kinetic Parameters for the G-Addition Step of Self-Splicing of *Anabaena* Pre-tRNA[a]

precursor	T (°C)	k_{cat}/K_m (M^{-1} min^{-1})	k_{cat} (min^{-1})	K_m (μM)
Anabaena	25	(2.7 ± 0.3) × 10^4 [b]	ND[c]	ND
	32	(4.6 ± 0.4) × 10^4 [b]	14 ± 4	240 ± 60
	37	(6.1 ± 0.7) × 10^4 [b]	ND	ND
Anabaena 5′-anti	32	(7.4 ± 0.2) × 10^2 [b]	0.38 ± 0.04	500 ± 30
Tetrahymena[d]	30	2.8 × 10^4	0.9 ± 0.1	32 ± 8
Tetrahymena[e]	30	1.5 × 10^3	0.044	29 ± 6
Tetrahymena[e]	42	1.5 × 10^4	0.46	30 ± 4

[a] Uncertainties in the precision of the rate constants for the *Anabaena* reactions are maximum values determined by independently fitting a line to the top and to the bottom of the error bar of each individual point on the k_{obs} vs [G] plot (such as that shown in Figure 4B). Uncertainties for *Tetrahymena* values are taken from the original sources, when given. [b] Second-order rate constant for reaction of precursor RNA and free guanosine, determined from the slope of plots of initial velocity vs [G], which were linear over the range used (e.g., insets in Figures 4B and 5B). [c] ND, not done. [d] Five millimolar $MgCl_2$, 30 mM Tris-HCl, pH 7.5, and 100 mM $(NH_4)_2SO_4$; guanosine was used as substrate (Bass & Cech, 1986). [e] Two millimolar $MgCl_2$, 30 mM Tris-HCl, pH 7.5, and 100 mM $(NH_4)_2SO_4$; GTP was used as substrate (Williamson et al., 1987).

Rate-Limiting Second Step. At early times during splicing in vitro there is a buildup of IVS-3′ exon, an intermediate in the splicing reaction which results from the cleavage of the 5′ splice site by guanosine (Figure 2A). At near-saturating guanosine concentrations, the first step of splicing is 90% complete in less than 0.25 min. This allows the rate of the second step to be measured by monitoring the disappearance of the intermediate at later times. At guanosine concentrations of 1000 and 2000 μM, both of which are above the K_m of guanosine, the observed rate for the second step is 0.3 min^{-1} (Figure 2D, 32 °C). The observed rate of the second step was independent of the concentration of guanosine (250–2000 μM).

Base-Pairing of Anticodon Stem Facilitates Splicing. The short internal guide sequence of the intron in this pre-tRNA led us to consider whether the nearby tRNA anticodon stem might contribute to reactivity. To test this, mutations were made in the tRNA to disrupt base-pairing in the anticodon stem, and the resulting mutant RNAs were assayed under standard splicing conditions (Figure 5A). The sequence and the proposed base-pairing of the anticodon stem of each mutant are indicated above the corresponding time course. Disrupting base-pairing by changing either the 5′ or the 3′ side of the anticodon stem decreased the rate of the first step of splicing. A 60-fold decrease in k_{cat}/K_m to 7.4 × 10^2 M^{-1} min^{-1} was measured for the 5′-anti mutant (Figure 5B). The 3′-anti change had an even greater effect (Table II). In addition, the 5′-anti mutant showed a decrease in the accumulation of IVS-3′ exon, indicating that the rate of the second step is less affected by this change in the anticodon stem than the rate of the first step. (If the rate of the second step had undergone a corresponding 60-fold rate reduction, the product distribution would have remained the same as that observed for the wild-type precursor.) The compensatory mutations, which restored base-pairing in the anticodon stem of the pre-tRNA, restored splicing activity to wild-type levels. The decrease in the accumulation of the splicing intermediate in this double mutant indicates an increase in the rate of the second step.

Smaller changes in the anticodon stem of the pre-tRNA were constructed by changing single bases, and splicing activities were tested under standard conditions (15 mM $MgCl_2$ both during the 15-min preincubation at 50 °C and during the splicing reaction at 32 °C). Disruption of the base pair in the center of the anticodon stem (G29C or C41G) decreased the rate of the first step of splicing (Table II). The compensatory double mutation (G29C:C41G), which restores base-pairing, restored splicing activity to wild-type levels. These results are similar to those obtained when all base-pairing in the anticodon stem was disrupted and then restored. When preincubation and splicing were carried out at 5, 2, or 1 mM Mg^{2+}, the single mutants were also splicing-defective and the compensatory double mutant again showed a wild-type level of activity (data not shown).

A Folding Mutant. In contrast to the mutants with base mismatches in the middle of the anticodon stem, the A31U and U39A mutants had splicing activities similar to that of the wild-type RNA at 15 mM Mg^{2+} (Table II). The time course of splicing was also measured at 5, 2, and 1 mM $MgCl_2$ during preincubation and splicing. A sample of the data is shown in Figure 6 (1 → 1 mM, where the numbers preceding and following the arrow give the $MgCl_2$ concentrations during the preincubation and the reaction, respectively). As the $MgCl_2$ concentration was lowered, the amount of the A31U RNA that reacted in 5 min decreased from 72% (15 mM $MgCl_2$) to 21% (2 mM $MgCl_2$) to ~1% (1 mM $MgCl_2$). The remainder failed to react even after 1 h. This defect was not rescued by the compensatory U39A mutation, and the U39A mutation by itself had no phenotype. These results indicate that nucleotide A31 has importance for splicing unrelated to its base-pairing with U39. In fact, our data provide no indication that A31 and U39, which are paired in the mature tRNA, are paired in the pre-tRNA.

Because the A31U mutation affected the fraction of reactive RNA rather than the rate of reaction of the active portion, it seemed likely to be affecting RNA folding. This hypothesis was tested by preincubation of the precursor RNA at 15 mM $MgCl_2$, followed by splicing at 2 or 1 mM $MgCl_2$. Preincubation at the higher $MgCl_2$ concentration largely suppressed the deleterious effect of the A31U mutation (e.g., 15 → 1 mM

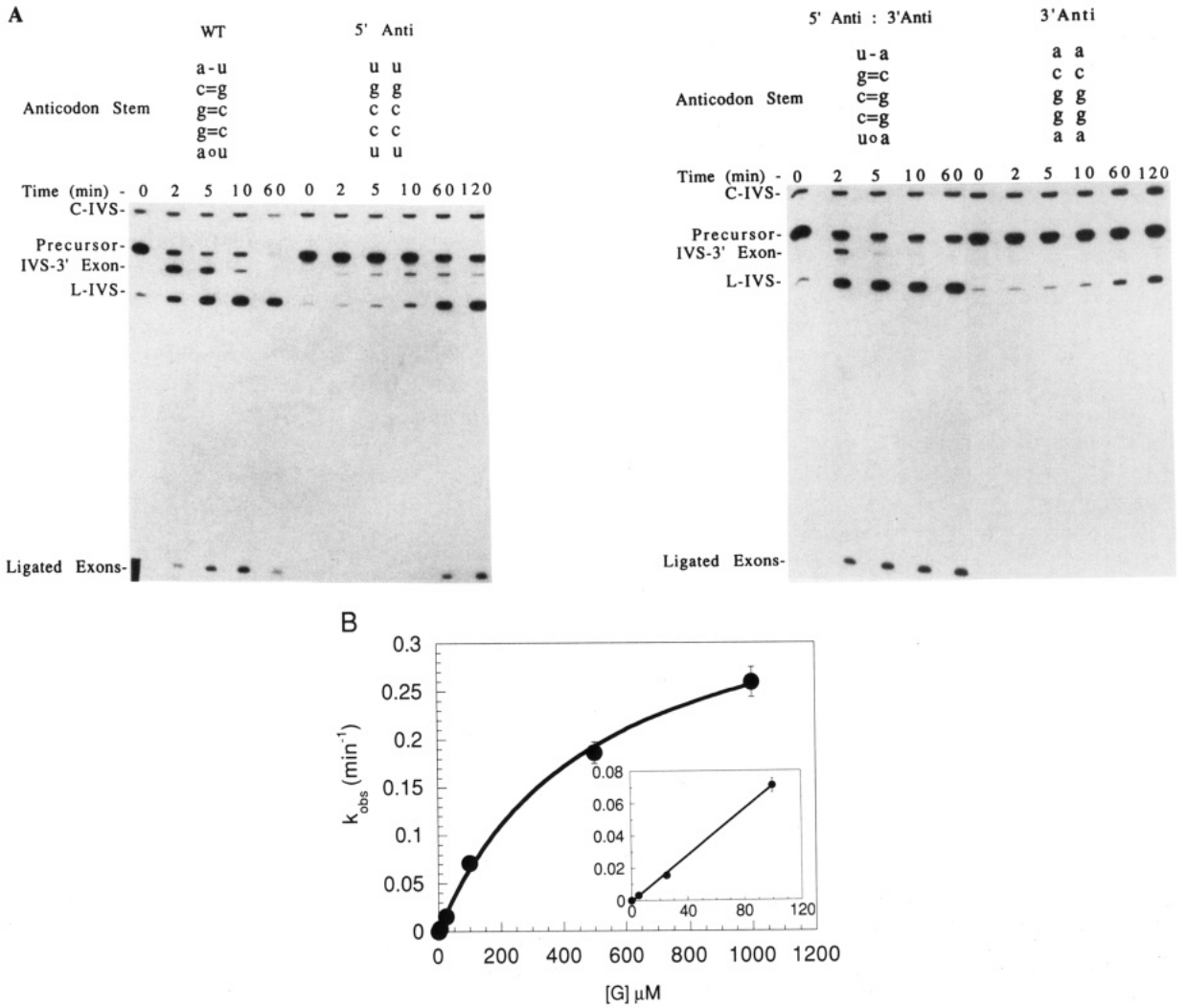

FIGURE 5: Anticodon stem mutants. (A) Products of splicing at 25 μM guanosine and 15 mM $MgCl_2$ for wild-type and anticodon stem mutants of *Anabaena* pre-tRNA. Above each time course is shown the base-pairing expected for the anticodon stem of each construct. The 5′-anti mutation changes the bases on the 5′ side of the anticodon stem to the same bases as are on the 3′ side of the stem, and the 3′-anti mutation changes the bases on the 3′ side of the anticodon to the same bases as are on the 5′ side of the stem. Both mutations completely disrupt base-pairing in the anticodon stem; (o) indicates base-pairing that may not occur in the precursor (see text). (B) Kinetic analysis of the first step of splicing of the 5′-anti mutant RNA. Each point was calculated from semi-log plots as in Figure 4.

Table II: Splicing of Anticodon Stem Mutants[a]

pre-tRNA	$t_{1/2}$ (min)[b]	k_{obs} (min^{-1})
wt	0.6	1
5′-anti	60	0.01
3′-anti	300	0.002
5′-anti:3′-anti	~1	~1
G29C	10	0.07
C41G	8	0.09
G29C:C41G	0.7	1
A31U	0.7	1
U39A	0.9	0.8
A31U:U39A	0.9	0.8

[a] Standard conditions of 15 mM $MgCl_2$ were used during both preincubation and splicing. Splicing was done with 25 μM guanosine, 32 °C. [b] At various times (0–60 min), products were analyzed by gel electrophoresis and quantitated by radioanalytic imaging, except 5′-anti:3′-anti, which was determined by visual comparison to wt RNA splicing based on data such as that shown in Figure 5. Half-life, $t_{1/2}$, refers only to the fraction of the molecules that reacted in the fast transition, typically 70–80% for the mutants and 85–90% for wt. Values have uncertainties of approximately ±10%, with the exception of those for 5′-anti:3′-anti, which could be as high as ±50%.

data in Figure 6). Thus, nucleotide A31 is important for correct RNA folding at the lower $MgCl_2$ concentrations, but is not required for activity once the RNA is properly folded.

DISCUSSION

A Small, Efficient Self-Splicing Intron. The $tRNA^{Leu}$ group I intron from *Anabaena* PCC7120 is an efficient self-splicing intron in vitro. Its k_{cat}/K_m is comparable to that of the *Tetrahymena* pre-rRNA group I intron, while its maximum rate for the first step of splicing at high concentrations of G (k_{cat}) is about 15-fold higher (Table I). The yeast mitochondrial cytochrome *b* intron 1 and the three bacteriophage T4 pre-mRNA introns all have values of k_{cat} less than or equal to that of the *Tetrahymena* intron, even when assayed at a $MgCl_2$ concentration and a temperature (37–60 °C) optimized for each RNA (Hicke et al., 1989; Schroeder et al., 1991). That such a small intron should splice so rapidly is surprising, because previous studies of other group I introns indicated that deletion of regions which are missing in the *Anabaena* group I intron have deleterious effects on catalytic activity (Price et al., 1985; Barfod & Cech, 1988; Doudna & Szostak, 1989; Beaudry & Joyce, 1990; van der Horst et al., 1991). Furthermore, the modest $MgCl_2$ and NaCl concentrations required for optimal splicing of the *Anabaena* pre-tRNA and retention of activity at elevated temperatures do not indicate a destabilized intron. As described in the next section, the high splicing efficiency may be aided by the structure of the mature tRNA exons.

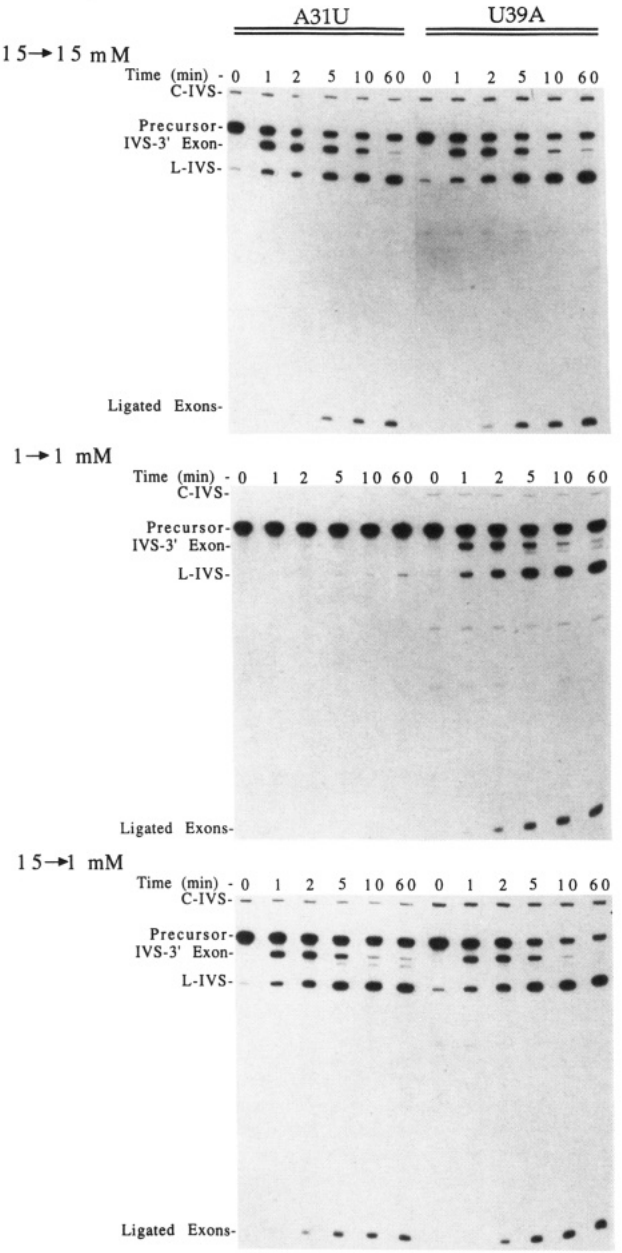

FIGURE 6: A folding mutant. The A31U mutant pre-tRNA (left-hand six lanes of each panel) requires high $MgCl_2$ concentration for proper folding during preincubation at 50 °C, but 1 mM Mg^{2+} is sufficient for its splicing at 32 °C. The U39A mutant (right-hand six lanes of each panel) splices well under all three conditions. The notation 15 → 1 mM indicates that 15 mM $MgCl_2$ was present during preincubation at 50 °C and was then diluted to 1 mM $MgCl_2$ prior to the addition of guanosine to initiate splicing at 32 °C; 15 → 15 mM and 1 → 1 mM, the indicated $MgCl_2$ concentration was present during both preincubation and splicing.

Splicing of the *Anabaena* pre-tRNA is particularly straightforward. The product distribution is much simpler than with the *Tetrahymena* pre-rRNA, with its multiple circularization sites (Inoue et al., 1986). In addition, most of the population of pre-tRNA reacts in a single first-order transition. This is in contrast to the *Tetrahymena* pre-rRNA, where a variable fraction (often ~1/2) of the molecules splice in the fast transition [Barfod & Cech, 1989; Woodson & Cech, 1991; see also Tanner and Cech (1985)]. We interpret this as evidence that the *Anabaena* pre-tRNA is more homogeneous structurally, when it is properly renatured (Figure 2B).

How well does the *Anabaena* intron bind guanosine? The *Anabaena* splicing reaction has $K_m = 240 \pm 60$ μM (32 °C), much higher than the $K_m \cong 30$ μM measured for the *Tetrahymena* splicing reaction (30 °C). However, a recent analysis of the equilibrium dissociation constant for G for an enzymatic form of the *Tetrahymena* intron gave $K_d^G = 190 \pm 30$ μM (30 °C; McConnell et al., 1993). Thus, it appears that $K_m \neq K_d$ for *Tetrahymena* pre-rRNA splicing, a situation which is thought to result from the splicing rate being limited by the chemical step at low [G] and a conformational change at high [G]. In contrast, for the *Anabaena* reaction there is evidence that $K_m = K_d^G$ (see below). Comparing $K_d^G = 190 \pm 30$ μM for the *Tetrahymena* intron with our estimate of $K_d^G = 240 \pm 60$ μM for the *Anabaena* intron leads to the conclusion that these two introns bind guanosine with similar affinity.

Some evidence that $K_m = K_d^G$ comes from the 5′-anti mutant. Because $K_m = (k_{-1} + k_{cat})/k_1$, K_m will equal K_d only if $k_{cat} \ll k_{-1}$, where

$$\text{RNA} + \text{G} \underset{k_{-1}}{\overset{k_1}{\rightleftharpoons}} \text{RNA·G} \xrightarrow{k_{cat}} \text{products}$$

The 5′-anti mutant has a value of k_{cat} 60-fold lower than that of the wild-type RNA, but it has a very similar value of K_m. The insensitivity of K_m to a decrease in k_{cat} provides evidence that $k_{cat} \ll k_{-1}$, so K_m is expected to equal K_d.

The second-order rate constant for reaction of free G and free precursor RNA, k_{cat}/K_m, is similar for the *Anabaena* and *Tetrahymena* precursors. This rate constant is thought to be limited by the actual chemical step in the case of the *Tetrahymena* pre-rRNA (Legault et al., 1992). We propose that k_{cat}/K_m for *Anabaena* pre-tRNA splicing may also be limited by the chemical step and that the similarity of the values of k_{cat}/K_m for these two precursors (Table I) indicates that these introns accomplish the chemistry of G-addition with similar efficiency.

The overall splicing reaction requires not just G-addition at the 5′ splice site but also exon ligation. This second step is rate-limiting at high G concentrations, as seen previously for the *Ankistrodesmus* intron (Davila-Aponte et al., 1991). One possible explanation was that blockage of the G-binding site by exogenous guanosine prevents the 3′ splice site G from entering. This possibility now seems unlikely, because the rate of exon ligation was not inhibited by increasing concentrations of G. The second step of splicing increased more dramatically than the first with increasing temperature (Figure 1C) or NaCl concentration (data not shown), which may indicate a conformational change in the intron between the first and second step of splicing. This conformational change may be rate-limiting for exon ligation.

Collaboration of Intron and tRNA Structures. We have become accustomed to thinking that the catalytic activity of group I introns resides within the intron moiety. In the case of the *Anabaena* system, RNA structure in the exons away from the splice sites also contributes substantially to catalysis. The 5′-anti and 3′-anti mutations, which disrupted the tRNA anticodon stem, decreased the rate of splicing (60-fold decrease in k_{cat}/K_m for 5′-anti). The mutations are physically distant from the guanosine binding site in P7, and the similar K_m for the 5′-anti mutant provides direct evidence that G binding is not much affected. (The 2-fold increase in K_m may indicate that P1 is not docked into the catalytic core in the 5′-anti mutant, a conclusion derived from studies with the *Tetrahymena* ribozyme; McConnell et al., 1993.) Instead of an effect on the G-site, we propose that the anticodon stem may stabilize the exceptionally short P1 helix, which would then become unpaired in the anticodon stem mutants and therefore would not be cleaved by guanosine. The activities of the 5′-anti and G29C mutants are restored by compensatory changes in the other half of the anticodon stem, showing that this structure rather than its exact sequence is important for activity. The

special case of the A31U mutant will be discussed later.

How might the anticodon stem stabilize P1? Initially we favored the idea that the anticodon stem might be stacked on P1. However, Michel and Westhof (1990) have proposed that P2 stacks on P1 in this subclass of group I introns, with an interaction between the GAAA hairpin loop of P2 and the P8 stem serving to position P1 for cleavage. Our recent mutagenesis data support the Michel–Westhof proposal (A. J. Zaug and T. R. Cech, unpublished results). If P2 is stacked on P1, then the anticodon stem is presumably oriented in some other manner. Simply by keeping the 5′ exon in proximity to the IGS, the anticodon stem could help reduce the entropic cost of P1 duplex formation.

Another possible role of the anticodon stem might be to "tie up" the nucleotides in P1, preventing unfavorable base-pairing or other interactions which could inhibit splicing (Woodson & Cech, 1991). In the absence of a paired anticodon stem, nucleotides 29–34 of the tRNA precursor might pair with nucleotides 69–74 of the T-loop of the tRNA (see Figure 1B), an interaction that would compete with the formation of the P1 duplex. While this interaction could be responsible for the slower rate of splicing observed with the 3′-anti mutant, the 5′-anti mutation was also deleterious, and we find no convincing alternative pairing for the 5′-anti RNA. Thus, we propose that the anticodon stem contributes positively to splicing, perhaps in addition to prevention of inhibitory interactions.

Experiments in which $MgCl_2$ concentration was varied during preincubation and the splicing reaction indicated that the mutations affect G-addition by different mechanisms. The G29C, C41G, and U39A mutants, like the wild-type precursor, showed similar rates of reaction with a variety of preincubation–reaction protocols. This behavior suggests that the mutants are not defective in overall folding, but rather that the folded state is relatively unreactive. In contrast, the A31U mutant was exceptionally Mg^{2+}-sensitive, but high Mg^{2+} was required mainly during the preincubation rather than the reaction itself. For example, the 15 → 1 mM combination (preincubation → reaction) was almost as good as the 15 → 15, and was far better than the 1 → 1 (Figure 6). Such behavior suggests that the mutation affects overall folding and that once the RNA is folded, the A31U mutation is almost neutral.

In conclusion, splicing of *Anabaena* pre-tRNA requires the collaboration of two RNA structures. The intron folds to provide the active site for splicing, and the tRNA anticodon stem serves an important auxiliary role, perhaps stabilizing the short P1 duplex that contains the 5′ splice site. The current analysis of the role of the tRNA exons was restricted to the anticodon stem. Other portions of the tRNA structure, such as the tertiary interaction between the D-loop and T-loop and the base-pairing in the acceptor stem, may also contribute to efficient splicing of this intron.

ACKNOWLEDGMENT

This work would not have been possible without the help of David Shub, who provided pXAb-107 and helpful discussions. We thank Dan Herschlag and Tim McConnell for comments on the manuscript. We also thank Anne Gooding for synthesis of DNA and RNA oligonucleotides and Alice Sirimarco for preparation of the manuscript.

REFERENCES

Barfod, E. T., & Cech, T. R. (1988) *Genes Dev. 2*, 652–653.
Barfod, E. T., & Cech, T. R. (1989) *Mol. Cell. Biol. 9*, 3657–3666.
Bass, B. L., & Cech, T. R. (1986) *Biochemistry 25*, 4473–4477.
Beaudry, A. A., & Joyce, G. F. (1990) *Biochemistry 29*, 6534–6539.
Burke, J. M., Belfort, M., Cech, T. R., Davies, R. W., Schweyen, R. J., Shub, D. A., Szostak, J. W., & Tabak, H. F. (1987) *Nucleic Acids Res. 15*, 7217–7221.
Cech, T. R., & Bass, B. L. (1986) *Annu. Rev. Biochem. 55*, 599–629.
Cech, T. R., Herschlag, D., Piccirilli, J. A., & Pyle, A. M. (1992) *J. Biol. Chem. 267*, 17479–17482.
Chu, F. K., Maley, G. F., West, D. K., Belfort, M., & Maley, F. (1986) *Cell 45*, 157–166.
Davenloo, P., Rosenberg, A. H., Dunn, J. J., & Studier, F. W. (1984) *Proc. Natl. Acad. Sci. U.S.A. 81*, 2035–2039.
Davies, R. W., Waring, R. B., Ray, J. A., Brown, T. A., & Scazzochio, C. (1982) *Nature 300*, 719–724.
Davila-Aponte, J. A., Huss, V. A. R., Sogin, M. L., & Cech, T. R. (1991) *Nucleic Acids Res. 19*, 4429–4436.
Doudna, J. A., & Szostak, J. W. (1989) *Mol. Cell Biol. 9*, 5480–5483.
Doudna, J. A., Cormack, B. P., & Szostak, J. W. (1989) *Proc. Natl. Acad. Sci. U.S.A. 86*, 7402–7406.
Garriga, G., & Lambowitz, A. M. (1984) *Cell 39*, 631–641.
Gott, J. M., Shub, D. A., & Belfort, M. (1986) *Cell 47*, 81–87.
Herschlag, D., & Cech, T. R. (1990) *Biochemistry 29*, 10159–10171.
Hicke, B. J., Christian, E. L., & Yarus, M. (1989) *EMBO J. 8*, 3843–3851.
Inoue, T., Sullivan, F. X., & Cech, T. R. (1986) *J. Mol. Biol. 189*, 143–165.
Kuhsel, M. G., Strickland, R., & Palmer, J. D. (1990) *Science 250*, 1570–1573.
Kunkel, T. A., Roberts, J. D., & Zakour, R. A. (1987) *Methods Enzymol. 154*, 367–382.
Legault, P., Herschlag, D., Celander, D. W., & Cech, T. R. (1992) *Nucleic Acids Res. 20*, 6613–6619.
McConnell, T., Cech, T. R., & Herschlag, D. (1993) *Proc. Natl. Acad. Sci. U.S.A.* (in press).
Michel, F., & Dujon, B. (1983) *EMBO J. 2*, 33–38.
Michel, F., & Westhof, E. (1990) *J. Mol. Biol. 216*, 585–610.
Michel, F., Jacquier, A., & Dujon, B. (1982) *Biochimie 64*, 867–881.
Michel, F., Hanna, M., Green, R., Bartel, D. P., & Szostak, J. W. (1989) *Nature 342*, 391–395.
Michel, F., Jaeger, L., Westhof, E., Kuras, R., Tihy, F., Xu, M. Q., & Shub, D. A. (1992) *Genes Dev. 6*, 1373–1385.
Nomiyama, H., Kuhara, S., Kukita, T., Otsuka, T., & Sakaki, Y. (1981) *Nucleic Acids Res. 9*, 5507–5520.
Price, J. V., Kieft, G. L., Kent, J. R., Sievers, E. L., & Cech, T. R. (1985) *Nucleic Acids Res. 13*, 1871–1889.
Pyle, A. M., Murphy, F. L., & Cech, T. R. (1992) *Nature 358*, 123–128.
Schroeder, R., von Ahsen, U., & Belfort, M. (1991) *Biochemistry 30*, 3295–3303.
Sogin, M. L., & Edman, J. C. (1989) *Nucleic Acids Res. 17*, 5349–5359.
Suh, R. R., & Waring, R. B. (1990) *Mol. Cell Biol. 10*, 2960–2965.
Tanner, N. K., & Cech, T. R. (1985) *Nucleic Acids Res. 13*, 7741–7758.
Van der Horst, G., & Tabak, H. F. (1985) *Cell 40*, 759–766.
Van der Horst, G., Christian, A., & Inoue, T. (1991) *Proc. Natl. Acad. Sci. U.S.A. 88*, 184–188.
Walstrum, S., & Uhlenbeck, O. C. (1990) *Biochemistry 29*, 10573–10576.
Waring, R. B., Scazzocchio, C., Brown, T. A., & Davies, R. W. (1983) *J. Mol. Biol. 167*, 595–605.
Wild, M. A., & Gall, J. G. (1979) *Cell 16*, 565–573.
Williamson, C. L., Tierney, W. M., Kerker, B. J., & Burke, J. M. (1987) *J. Biol. Chem. 262*, 14672–14682.
Woodson, S. A., & Cech, T. R. (1991) *Biochemistry 30*, 2042–2050.
Xu, M. Q., Kathe, S. D., Goodrich-Blair, H., Nierzwicki-Bauer, S. A., & Shub, D. A. (1990) *Science 250*, 1566–1570.